

Excellence in Chemistry Research

Announcing our new flagship journal

- Gold Open Access
- Publishing charges waived
- Preprints welcome
- Edited by active scientists



Meet the Editors of *ChemistryEurope*



Luisa De Cola

Università degli Studi
di Milano Statale, Italy



Ive Hermans

University of
Wisconsin-Madison, USA



Ken Tanaka

Tokyo Institute of
Technology, Japan

5-Styrylisoxazoles: π -Conjugated System with Fluorescent Properties and Bioactivity

Kirill S. Sadovnikov,^[a] Dmitry A. Vasilenko,^[a] Yulia A. Gracheva,^[a] Yuri K. Grishin,^[a] Vitaly A. Roznyatovsky,^[a] Victor A. Tafeenko,^[a] Nadezhda E. Astakhova,^[a] Ivan D. Burtsev,^[b] Elena R. Milaeva,^[a] and Elena B. Averina^{*[a]}

A simple two-step protocol for the synthesis of 3-aryl/hetaryl-4-nitro-5-styrylisoxazole was elaborated. A large series of novel 5-styrylisoxazoles (36 compounds) containing various substituents at positions 3 and 5 of isoxazole cycle was obtained. The title compounds revealed fluorescent properties in visible region, possessing emission maximum up to 610nm. The effect

of solvatochromism and chemosensor properties towards a number of metal cations were demonstrated. Cytotoxic activity against MCF-7 (breast carcinoma), HCT-116 (colon carcinoma), A549 (pulmonary carcinoma) and WI38 (fibroblasts from lung tissue) cell lines was tested and toxicity in the concentration range of 10–100 μ M was found for several compounds.

Introduction

Isoxazoles are an important class of *N,O*-heterocycles of considerable interest to medicinal chemistry and organic synthesis.^[1,2] Isoxazole motif has attracted increasing attention as a core of natural products (e.g. ibotenic acid, muscimol) and an important scaffold of compounds which demonstrate various types of biological activities, such as anticancer, antiviral, immunomodulatory, antimicrobial, anti-inflammatory, antifungal, and others.^[3] Also, it is known that 4-nitro-5-styrylisoxazoles, obtained from commercially available 3,5-dimethyl-4-nitroisoxazole, are widely used in organic synthesis due to their unique reactivity. Thus, styrylisoxazoles have been involved in enantioselective and diastereoselective reactions, such as the Michael addition of nucleophiles to the double bond,^[4] domino Michael/cyclization processes,^[5] [3+2]-cycloaddition^[6] and aza-Diels-Alder reactions.^[7] Another possible application of nitrosubstituted isoxazole moiety is their employment in the construction of π -conjugated systems with fluorescent properties. The combination of electron-acceptor 4-nitroisoxazole fragment with different donor aromatic rings using a vinyl group linker results in "push-pull" molecules that can be seen as attractive objects for the development of advanced functional materials and in the medicinal chemistry.^[8] In general, styryl dyes, including heterocycle containing structures, are important group of fluorophores due to their

synthetic availability, easy purification and useful physical or chemical properties such as light emission, photoelectric and photochemical activity, as well as bio-labelling and photosensitization.^[9] Nonetheless, photophysical properties of 4-nitro-5-styrylisoxazoles have been tested using only a few examples for 3-methyl substituted isoxazole derivatives.^[10] To our knowledge, 3-aryl-4-nitro-5-styrylisoxazoles have not yet been investigated as fluorescent chemical compounds.

Previously, we elaborated a novel approach to 3-aryl/hetaryl-4-nitroisoxazoles based on heterocyclization of aryl/hetaryl vinyl ketones upon the treatment with $C(NO_2)_4/Et_3N$ or *t*-BuONO/ H_2O . This method allows to obtain the target heterocycles in high yields in gram-scale quantities.^[11] Thus, in this work we employed this method for the synthesis of a large series of previously unknown 3-aryl-5-styryl-4-nitroisoxazoles bearing various substituents at positions 3 and 5 of the isoxazole ring, and the investigation of their photophysical properties and cytotoxicity.

Results and Discussion

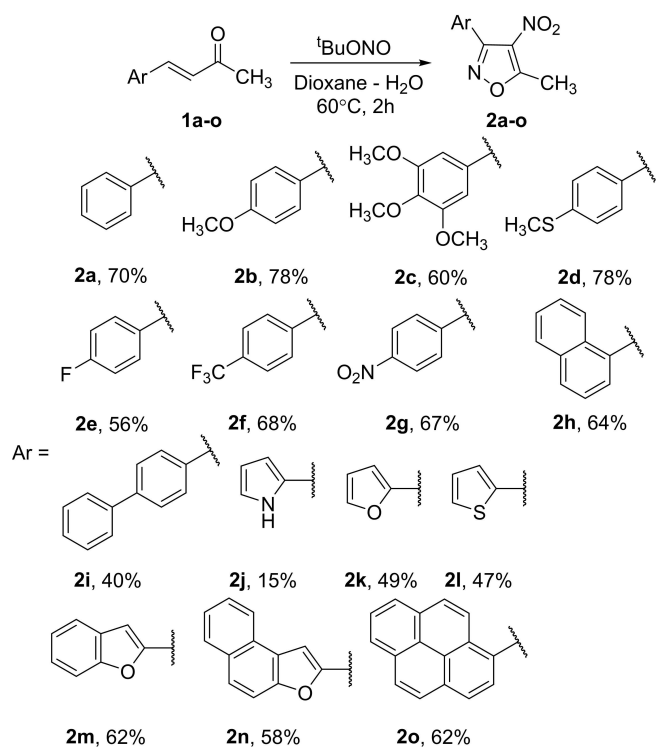
To obtain novel isoxazole-containing π -conjugated systems a wide range of 5-methyl-4-nitroisoxazoles **2a–o** were synthesized by our method.^[11] The reaction of heterocyclization of α,β -unsaturated ketones **1a–o** proceeded smoothly under standard conditions giving 4-nitroisoxazoles **2a–o** in good isolated yields (Scheme 1).

The next synthetic transformation of compounds **2a–o** included the Knoevenagel-type condensation involving methyl group at position 5 of isoxazole fragment. A brief optimization of the condensation conditions, including varying the base, solvent, reaction time and temperature, was carried out (see Table S1 in SI), and the best result was achieved using piperidine as a base and EtOH as a solvent. The reaction was completed in 2 h at 80°C or 24 h at room temperature. Refluxing in EtOH was used in the case of poor solubility of starting aldehydes or 4-nitroisoxazoles in the condensation reaction.

[a] Dr. K. S. Sadovnikov, Dr. D. A. Vasilenko, Dr. Y. A. Gracheva, Dr. Y. K. Grishin, Dr. V. A. Roznyatovsky, Dr. V. A. Tafeenko, N. E. Astakhova, Prof. Dr. E. R. Milaeva, Prof. Dr. E. B. Averina
Department of Chemistry
Lomonosov Moscow State University
Leninskie Gory, 1–3, Moscow 119991, Russia
E-mail: elaver@med.chem.msu.ru

[b] Dr. I. D. Burtsev
Emanuel Institute of Biochemical Physics
Russian Academy of Sciences
4 Kosygin st., Moscow 119334, Russia

Supporting information for this article is available on the WWW under <https://doi.org/10.1002/slct.202300830>



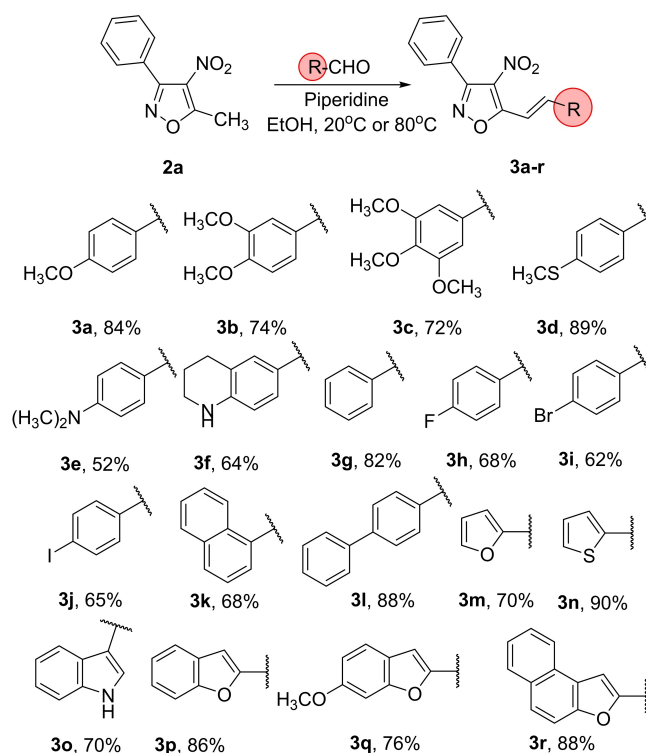
Scheme 1. Synthesis of 4-nitroisoxazoles 2a–o.

Under the optimized conditions, two series of novel 5-styrylisoxazoles with different aryl substituents in the styryl fragment (position 5) and at position 3 of the isoxazole cycle were obtained to evaluate the influence of the structure on photophysical properties.

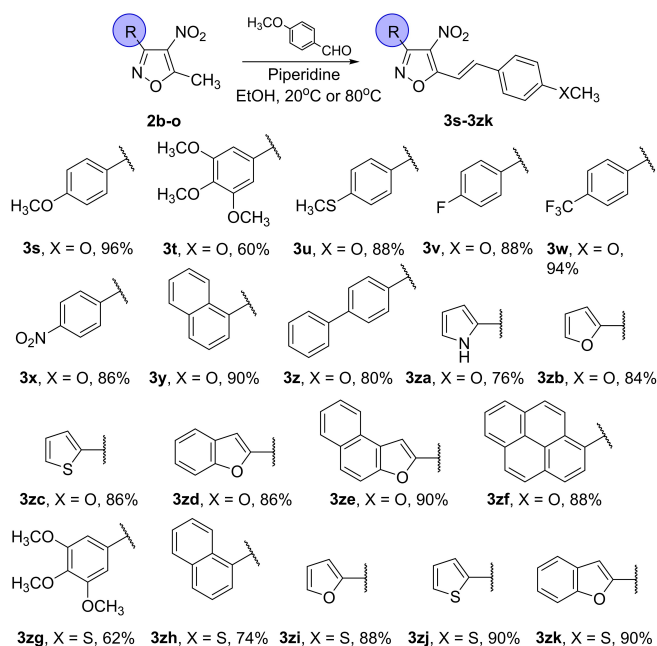
The first series of 5-styrylisoxazoles **3a–r** was synthesized from 3-phenyl-4-nitroisoxazole **2a** and aromatic aldehydes with halogens, alkoxy-, thioalkoxy-, amino- and phenyl groups in the aromatic rings, as well as aldehydes containing naphthyl or donor heterocyclic moieties were employed (Scheme 2). All aldehydes reacted with isoxazole **2a** affording condensation products **3a–r** in good yields, a slight decrease in the yields of compounds **3e** and **3i** is due to their low solubility in organic solvents.

The second series of 5-styrylisoxazoles was synthesized to examine the effect of aryl/hetaryl fragments at position 3 of the isoxazole ring on the fluorescent properties. For this purpose 5-methyl-4-nitroisoxazoles **2a–o** with a variety of aryl/hetaryl substituents were involved in the condensation reaction under standard conditions with *p*-anisaldehyde or *p*-(methylthio)benzaldehyde affording compounds **3s–3zk** in high yields (Scheme 3).

The photophysical properties of compounds **3a–3zk** were studied by UV-vis and fluorescence spectroscopy in CH_2Cl_2 at room temperature. Spectra of electronic absorption and emission were recorded; the absorption coefficients and fluorescence quantum yields were measured for all obtained compounds (Figure 1 and 2, Table 1 and 2).



Scheme 2. Synthesis of 3-phenyl-4-nitro-5-styrylisoxazole 3a–r.



Scheme 3. Synthesis of 3-aryl/hetaryl-4-nitro-5-styrylisoxazoles 3s–3zk.

For the most of 3-phenyl-5-styrylisoxazoles **3a–r** (the first series of compounds) the longest-wavelength absorption maxima lay in the visible region, at 390–508 nm, and the emission maxima lay in the range of 466–610 nm (also see

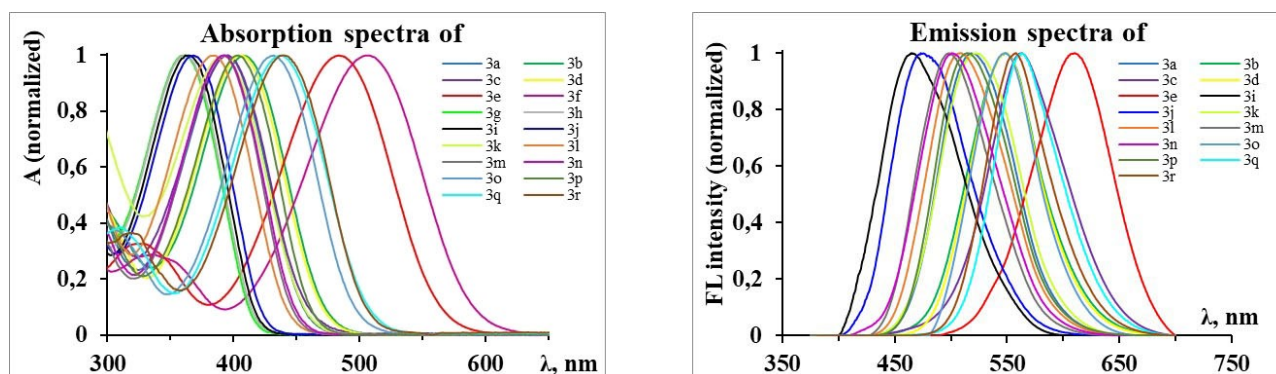
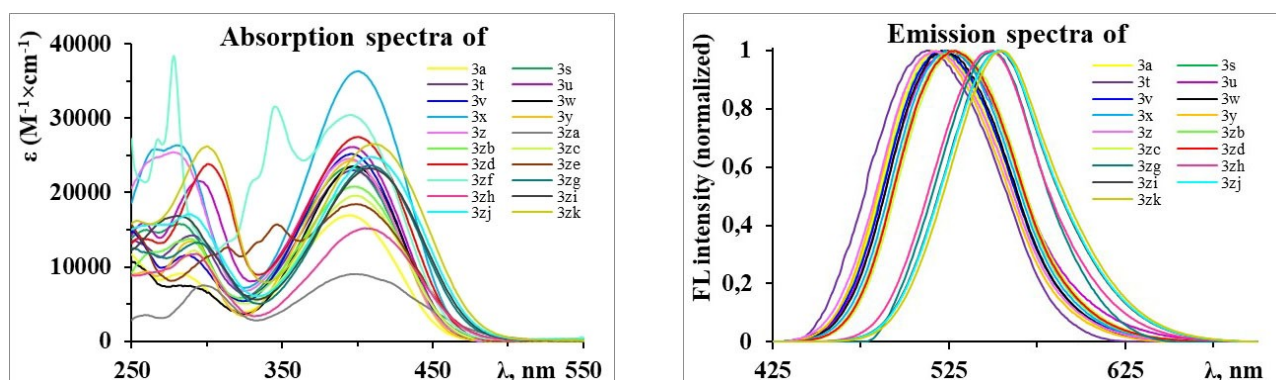
Figure 1. Absorption and emission spectra of compounds **3a–r**.Figure 2. Absorption and emission spectra for compounds **3a, 3s–3iz**.

Figure S3 and S4 in SI). Significantly, studied compounds **3a–r** are characterized by the large Stokes shifts (100–140 nm).

The series of isoxazoles (**3a, 3d, 3k, 3l, 3m, 3n, 3p–3r**), containing arylalkoxy-, alkylthioaryl-, polyaromatic groups as well as furyl or thienyl substituents in styryl moieties, are characterized by similar absorption bands in the region 390–410 nm. Amino groups in styryl fragments (**3e, 3f**) brings about more pronounced redshifts in absorption spectra (480–510 nm) than electron-donor -OMe or -SMe substituents. Also, the extension of π -conjugation in heterocycles **3k, 3l, 3p–3r** indicates the same effect. It should be noted that for arylamino substituted 5-styrylisoxazoles **3e,f** demonstrated the largest molar extinction coefficients ϵ of 31700 and 34400 $\text{M}^{-1}\text{cm}^{-1}$. As shown in Table 1 the electronic nature of substituents in the aromatic ring of the styryl fragment has a strong effect on the fluorescent properties. Thus, it was found that fluorescence in the visible region is not observed for phenyl substituted 5-styrylisoxazole **3g** as well as for styrylisoxazole **3h** bearing strong inductively electron withdrawing fluorine in the phenyl ring of styryl fragment. Considering compounds **3h–j**, containing *p*-(halogen)phenyl substituents, it should be mentioned that the quantum yields increase with a decrease in electronegativity of halogens. Important results were obtained for heterocycles **3d** and **3e**, which contain *p*-methylthio- and *p*-(dimethylamino)phenyl groups in styryl moieties. Thus, com-

pound **3d** is characterized by one of the highest fluorescence quantum yields in these series of 5-styrylisoxazoles. The longest wavelength maximum of the emission ($\lambda_{\text{em}}^{\text{max}}=610\text{ nm}$) and the highest molar extinction coefficient ($\epsilon=34400\text{ M}^{-1}\text{cm}^{-1}$) are observed for heterocycle **3e**, but this compound displays an extremely low quantum yield value of 0.1%. This fact can be explained by the presence of a strong resonance effect of the NMe_2 group: the zwitterionic form **3e'** makes a significant contribution to the structure of the excited state, that results in nonradiative transfer of energy and reduces the value of the quantum yield (Scheme 4).

It appeared that the incorporation of an *N*-methyltetrahydroquinoline fragment (isoxazole derivative **3f**) in styryl part led to the highest redshift maxima of absorption ($\lambda_{\text{abs}}^{\text{max}}=508\text{ nm}$), but was accompanied by almost total loss of emission in the visible region. Replacing aryl groups by *N*-, *O*-

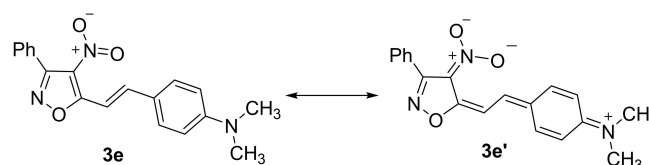
Scheme 4. Resonance structures of **3e**.

Table 1. Photophysical characteristics of 5-styrylisoxazoles **3 a-r** measured in CH₂Cl₂.

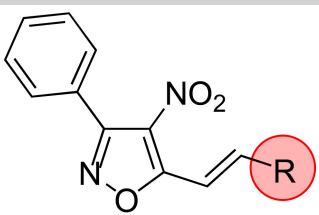
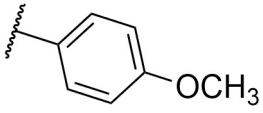
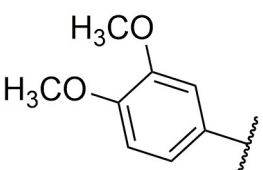
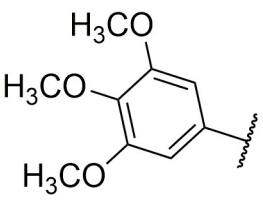
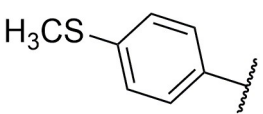
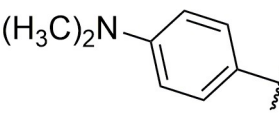
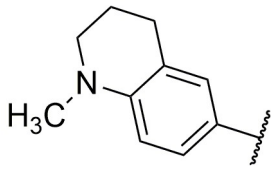
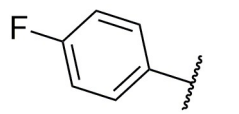
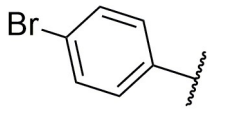
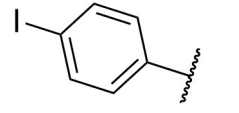
N	R	$\lambda_{\text{abs}}^{\text{max}}$ [nm]	$\lambda_{\text{emr}}^{\text{max}}$ [nm] ^[a]	$\Delta\nu$, [cm ⁻¹]	ϵ , [M ⁻¹ cm ⁻¹]	ψ , %
		 <p style="text-align: center;">3a-r</p>				
3a		386	518	6602	16900	0.6
3b		408	548	6262	26300	0.5
3c		393	563	7683	18800	0.2
3d		407	549	6355	26000	3.6
3e		484	610	4268	34400	0.1
3f		508	660	4534	31700	0.05
3g	Ph	360	–	–	21400	–
3h		360	–	–	24000	–
3i		364	466	6013	23500	0.1
3j		368	476	6166	28000	0.2

Table 1. continued

3a-r

N	R	$\lambda_{\text{abs}}^{\text{max}}$ [nm]	$\lambda_{\text{emr}}^{\text{max}}$ [nm] ^[a]	$\Delta\nu$, [cm ⁻¹]	ϵ , [M ⁻¹ cm ⁻¹]	ψ , %
3k		392	523	6390	14400	1.5
3l		382	515	6761	24500	2.2
3m		392	489	5060	23800	0.3
3n		393	500	5445	18700	0.1
3o		432	548	4900	25700	0.3
3p		403	514	5359	23100	2.9
3q		438	563	5069	29300	1.2
3r		440	557	4774	26200	4.3

[a] The longest-wavelength absorption maxima.

S-heteroaromatic cycles in the styryl fragment (**3m–3o**) does not lead to noticeable changes in the emission spectra, however, the extension of the π -system results in bathochromic

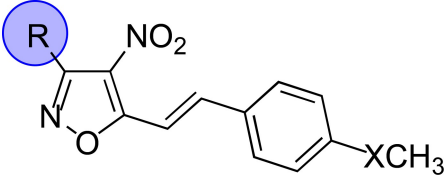
shifts of the emission bands and an increase in quantum yields (compounds **3k, l, p–r**). Thus, compound **3r** with a naphthofur-

Table 2. Photophysical characteristics of 3-aryl/hetaryl-4-nitro-5-styrylisoxazole **3a**, **3s-3zk** measured in CH₂Cl₂.

3a, 3s-3zk

N	R	X	$\lambda_{\text{abs}}^{\text{max}}$ [nm]	$\lambda_{\text{emv}}^{\text{max}}$ [nm] ^[a]	$\Delta\nu$, [cm ⁻¹]	ϵ , [M ⁻¹ cm ⁻¹]	ψ , %
3a	Ph	O	386	518	6602	16900	0.6
3s		O	395	522	6159	23100	0.5
3t		O	397	512	5658	23100	0.2
3u		O	398	525	6078	24100	0.5
3v		O	396	521	6059	25000	0.5
3w		O	398	523	6005	23600	0.8
3x		O	398	526	6114	38700	0.8
3y		O	397	516	5809	24200	1.1
3z		O	395	519	6049	24400	0.9
3za		O	400	–	–	9100	–
3zb		O	398	528	6186	20900	0.9

Table 2. continued



3a, 3s-3zk

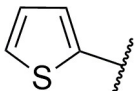
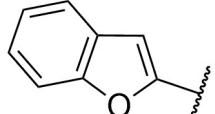
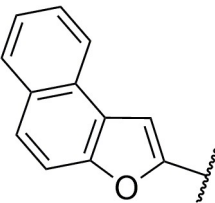
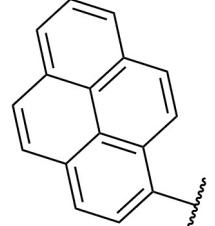
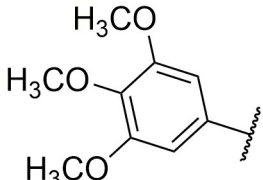
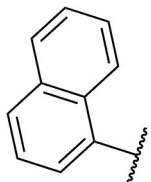
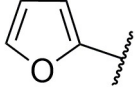
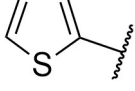
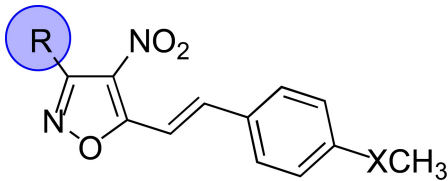
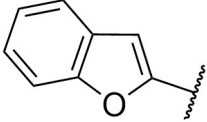
N	R	X	$\lambda^{\max}_{\text{abs}}$ [nm]	$\lambda^{\max}_{\text{em}}$ [nm] ^[a]	ΔV , [cm ⁻¹]	ϵ , [M ⁻¹ cm ⁻¹]	ψ , %
3zc		O	397	530	6321	19700	0.9
3zd		O	400	530	6132	25200	1.2
3ze		O	398	–	–	18600	–
3zf		O	396	–	–	30600	–
3zg		S	408	550	6328	23700	1.0
3zh		S	405	549	6476	15400	4.6
3zi		S	409	553	6367	23400	3.9
3zj		S	409	553	6367	25000	3.4

Table 2. continued							
 3a, 3s-3zk							
N	R	X	$\lambda_{\text{abs}}^{\text{max}}$ [nm]	$\lambda_{\text{em}}^{\text{max}}$ [nm] ^[a]	ΔV , [cm ⁻¹]	ϵ , [M ⁻¹ cm ⁻¹]	ψ , %
3zk		S	410	555	6372	26600	3.8

[a] The longest-wavelength absorption maxima.

an substituent is characterized by the highest quantum yield (4.3%) and a long wave maximum of emission at 557 nm.

For a deeper understanding of the photophysical properties of 3-phenyl-5-styrylisoxazoles **3a-r** the DFT calculations for compounds **3a**, **3d**, **3e**, **3g** and **3h** were performed. All calculations were accomplished by the Orca 4.2.1 software package^[12] with B3LYP/G TZVP method^[13] and summarized in the Figure 3. The highest occupied molecular orbitals (HOMOs) for structures **3a**, **3d**, **3e**, **3g**, **3h** are distributed over styryl fragment and partly isoxazole, while their lowest unoccupied molecular orbitals (LUMOs) are mainly located on the nitro group and on the styryl double bond. It should be noted that phenyl substituent at position 3 of isoxazole ring of compounds **3a**, **3d**, **3e** with fluorescent properties is not involved in the electron distribution, while HOMOs of heterocycles **3g**, **3h** without emission in visible region are located through

whole conjugated system. As can be seen from Figure 3, the value of energetic gap decreases in the sequence of 5-styrylisoxazoles **3g**→**3h**→**3a**→**3d**→**3e** and these results correlate with redshift maxima of absorption and emission in this series of compounds.

To obtain further insight into the relationship between the structure and photophysical properties of 5-styrylisoxazoles we investigated the second series of compounds **3a**, **3s-3zk** with the variation of the substituents at position 3 of the isoxazole cycle. The main absorption maxima for the series of isoxazoles with 5-(*p*-methoxyphenyl)styryl fragment (**3a**, **3s-3zf**) have close values in the range of 395–400 nm, and compound **3x** with the *p*-NO₂ group in 3-aryl substituent has the largest hyperchromic effect ($\epsilon = 38680 \text{ M}^{-1} \text{ cm}^{-1}$). For 3-arylisoxazoles with *p*-(methylthiophenyl)vinyl moiety, there is a slight shift of the absorption maxima to the long-wavelength region up to

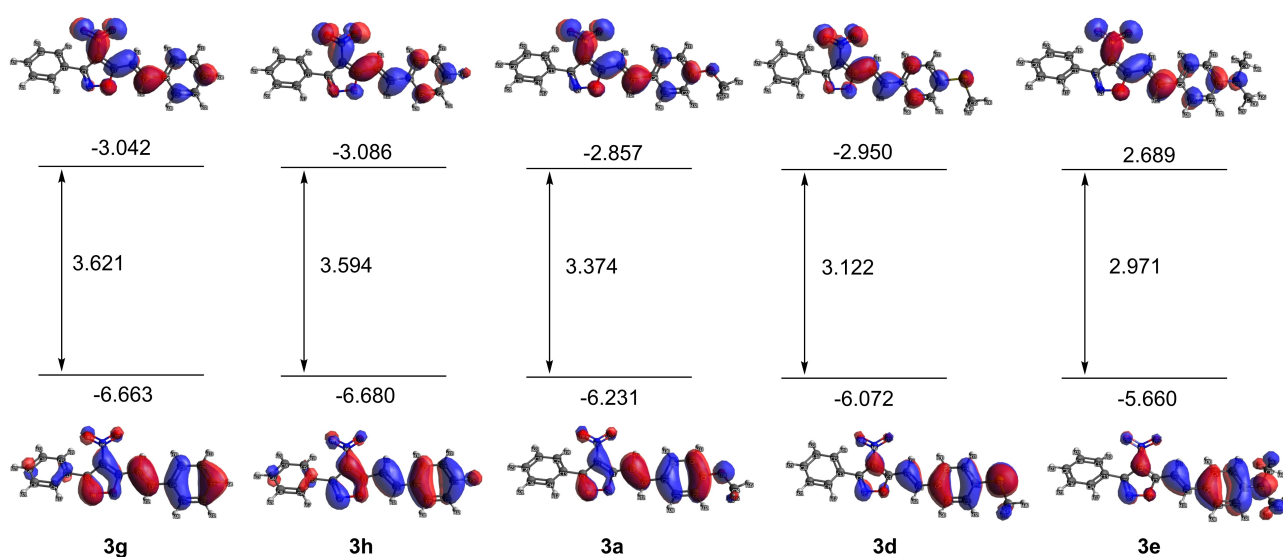


Figure 3. Frontier molecular orbitals (FMOs) of **3a**, **3d**, **3e**, **3g** and **3h**, their energies (eV) and energy difference (ΔE , eV).

410 nm, but the substituents at position 3 of isoxazole cycle do not significantly affect the absorption maximum.

Two series of the 3-aryl-5-styrylisoxazoles **3s–3zf** and **3zg–3zk**, differing in the nature of the 5-aryl/hetaryl substituents, exhibit the emission maxima ranging from 512 to 530 nm and from 549 to 555 nm, respectively. It should be noted that, as well as in absorption spectra, the position of the fluorescence maxima bands weakly depends on the substituents at position 3, and they are specified by the nature of the 5-styryl fragment. Increasing the length of π -system in position 3 of isoxazole cycle leads to an increase in the quantum yield up to 4.6% (compounds **3y**, **3z**, **3zd**, **3zh** and **3zk**). However, the incorporation of the naphthofuran or pyrene fragments into position 3 of heterocycles **3ze** and **3zf** completely quenches the fluorescence in visible region.

To explain a slight impact of the aromatic ring at position 3 of isoxazole on the photophysical properties we performed the geometrical optimization (DFT B3LYP/G TZVP) for compounds **3a** and **3zb** (Figure 4, 5). As shown in Figure 4, the phenyl ring at position 3 of isoxazole **3a** and 4-nitroisoxazole unit do not lay in the same plane (dihedral angle: 39.5°), therefore, there is no effective conjugation between them. This result additionally confirms the weak influence of the extension of the π -system and the absence of the mesomeric effect of substituents in the aromatic ring (position 3) on the fluorescent properties. In this case, the cumulative inductive effect of the substituent at position 3 plays a more important role.

In contrast, according to quantum chemical calculations (DFT B3LYP/G TZVP), the compound **3zb** bearing 3-furyl substituent has almost completely planar structure (Figure 5), that results in the extension of π -conjugated system. Indeed, the presence of donor heteroaromatic substituents at position 3 of the isoxazole ring leads to slight redshifts maxima of emission and an increase in the quantum yields for compounds **3zb–3zd** and **3zi–3zk**. On the other hand, 3-(pyrrol-2-yl)-isoxazole **3za** shows the lowest quantum yield that can be explained by the strong electron-donor properties of the pyrrole ring, and as a consequence, less effective intramolecular charge transfer.

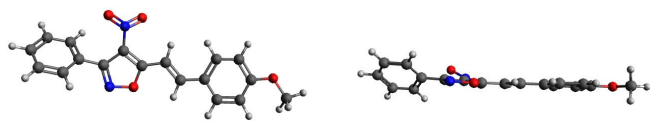


Figure 4. Calculations of the geometry of 5-styrylisoxazole molecules with an exemplary heterocycle **3a** by DFT method (B3LYP/G TZVP).

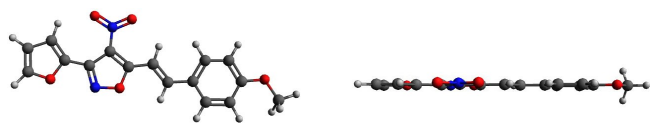


Figure 5. Calculations of the geometry of 5-styrylisoxazole molecules with an exemplary heterocycle **3zb** by the DFT method (B3LYP/G TZVP).

Differences in the structure of isoxazoles bearing aromatic ring or 5-membered heterocycles at position 3 of isoxazole ring are also confirmed by X-ray diffraction studies of compounds **3zb** and **3zh**. According to the X-ray analysis compound **3zb** is nearly planar, and the dihedral angle between the furan and isoxazole heterocycles is equal to 12.2° (Figure 6). Meanwhile, the dihedral angle between the naphthalene and isoxazole in compound **3zh** is equal to 62.0° (Figure 6), as a result, aromatic substituent at the position 3 of isoxazoles has a weak influence on the π -electron system of this chromophore.

Photostability of the obtained styrylisoxazoles were investigated using compound **3zh** as a model substrate. In this study the solution of **3zh** in CDCl_3 was irradiated with near ultraviolet light (365 nm) for 5, 15, 30 and 60 min and the changes in the structure of the compound were recorded using NMR ^1H spectroscopy. It was found that the photoirradiation of **3zh** in CDCl_3 induced slow E/Z-photoisomerization typical for styryl dyes.^[14] After 60 min of irradiation the ratio of E and Z isomers was 1:0.31 (Figure 7 and Figure S5 in SI). The photoisomerization was also reflected in fluorescent properties and the intensity of fluorescence of **3zh** taken as a solution in DCM (with the maximum at 549 nm) gradually decreased after the irradiation with light of 365 nm for 10, 30, 60 min (Figure 8).

Also the kinetic of fluorescence decay was studied for styrylisoxazole derivative **3zh** with the highest quantum yield of this series of compounds (Figure 9). It was found that the decay of the excited state of **3zh** has monoexponential decrease in emission spectrum with a short fluorescent lifetime (0.9 ns).

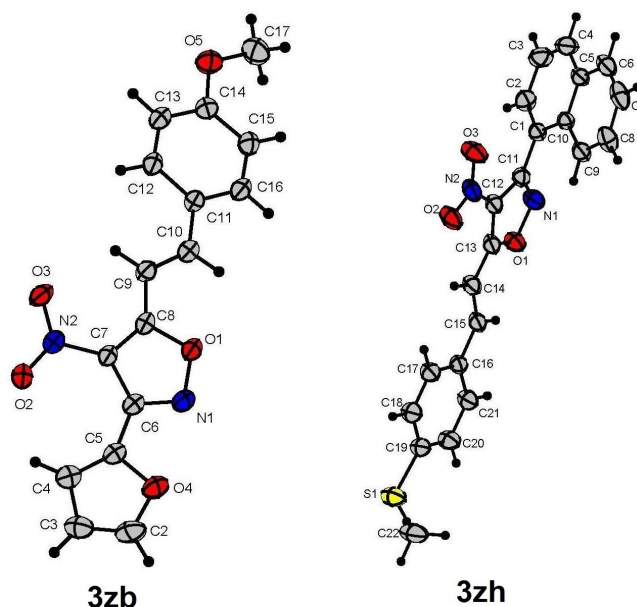


Figure 6. The molecular structures of **3zb** and **3zh**, showing the atom-numbering scheme. Displacement ellipsoids are drawn at the 50% probability level, H atoms presented as spheres with arbitrary radii.

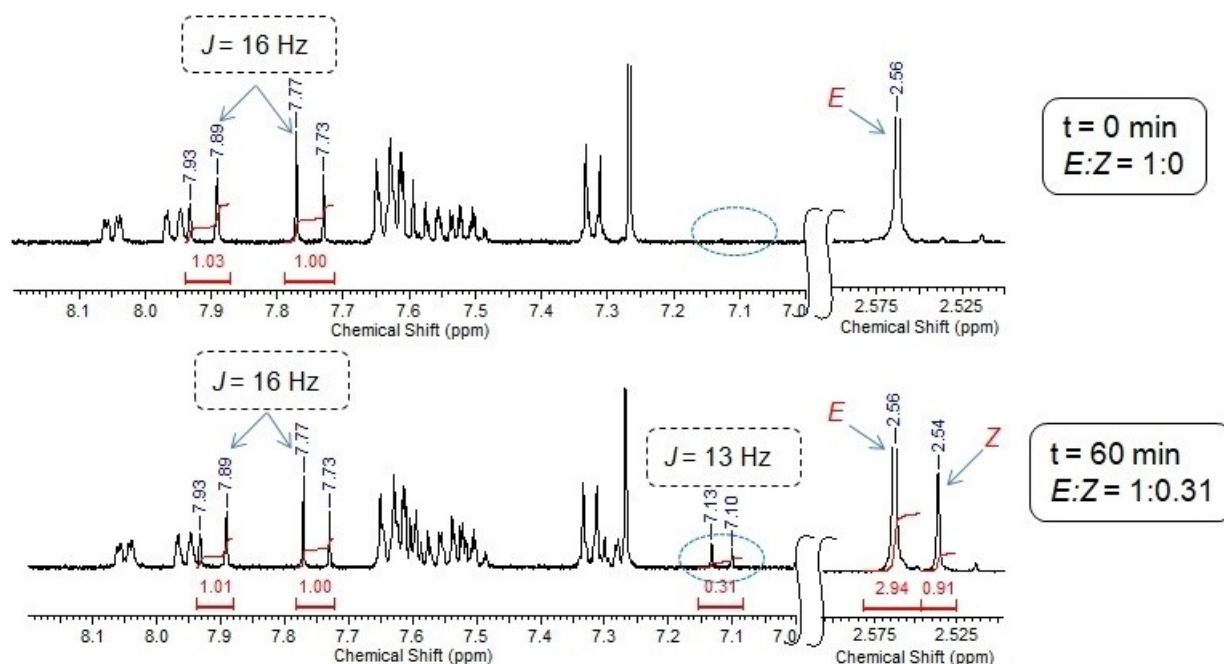


Figure 7. ^1H NMR (400 MHz, CDCl_3) of **3zh** before and after irradiation of a sample with light with wavelength of 365 nm.

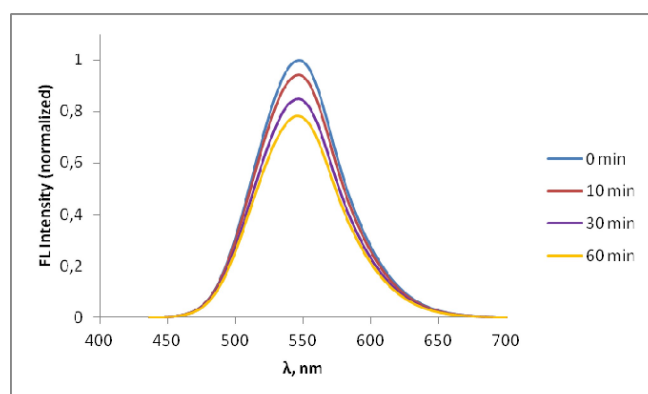


Figure 8. The change in the intensity of **3zh** after long-term irradiation with light with wavelength of 365 nm.

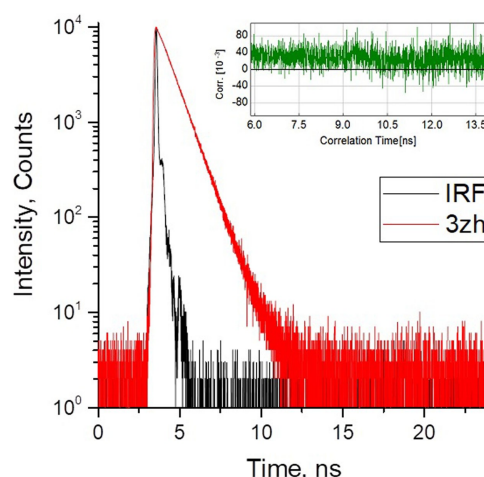


Figure 9. Fluorescence lifetime decay curve of **3zh** in dichloromethane ($\lambda_{\text{exc}} = 375$ nm, $\lambda_{\text{reg}} = 540$ nm).

Solvatochromism and sensor properties

To investigate the solvatochromic effect of 5-styrylisoxazoles we measured the absorption and fluorescence spectra in various solvents for compound **3zh** with one of the long-wavelength fluorescence maximum and the highest quantum yield. It was observed that the solvent has little or no impact on the absorption maxima. Meanwhile, styrylisoxazole **3zh** exhibited pronounced positive fluorescence solvatochromism with a bathochromic shift up to 164 nm in the solvents range from benzene to DMSO. (Table 3, Figure 10). In addition, the influence of the solvent polarity on photophysical properties of fluorophore **3zh** was shown by plotting the dependence of Stokes shift of dye versus the orientation polarizability (Δf) in accordance with the Lippert-Mataga equation.^[15] A linear

relationship over the whole range of solvent polarity (Figure 11) with the exception of

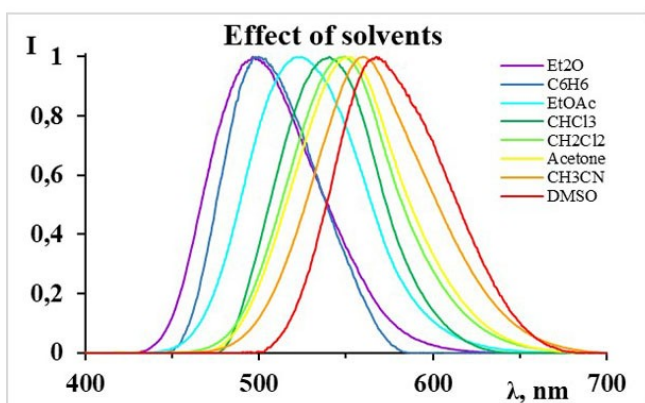
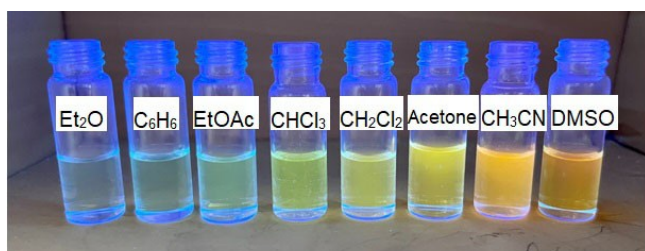
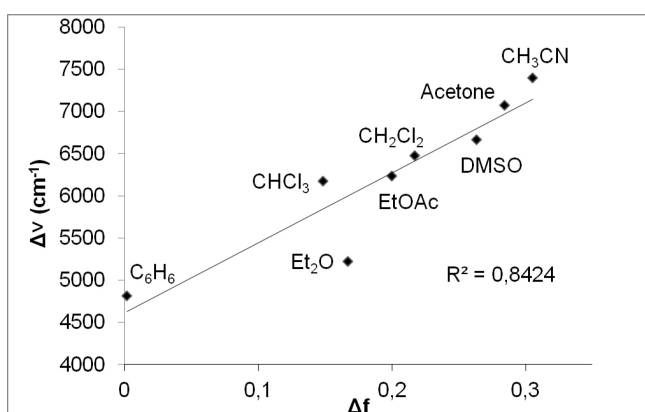
Et_2O was obtained with acceptable regression coefficients ($R^2 = 0.97$) (see Figure S7 in SI).

Thus, the positive emission solvatochromic shift was observed due to physical factors of solvents. Deviation from linearity in the case of Et_2O could probably be because of the specific interactions between the lone pair of solvent and electrophilic double bond of styrylisoxazole **3zh**.

Taking into account the possibility of coordination of metals with the isoxazole moiety^[16] we probed the chemosensor properties of 5-styrylisoxazoles. For this purpose

Table 3. Effect of solvents on the photophysical properties of compound **3zh** and solvents orientation polarizability (Δf).

Solvent	$\lambda_{\text{abs}}^{\text{max}}$ [nm]	$\lambda_{\text{emr}}^{\text{max}}$ [nm]	$\Delta\nu$, [cm ⁻¹]	ϵ	n_D	Δf
Et ₂ O	392	496	5349	2,27	1,5011	0,001642
C ₆ H ₆	403	500	4814	4,33	1,3524	0,166749
EtOAc	395	524	6232	4,81	1,4458	0,148295
CHCl ₃	405	540	6173	6,02	1,3724	0,199635
CH ₂ Cl ₂	405	549	6476	8,93	1,4241	0,217137
Acetone	397	552	7073	20,70	1,3587	0,284307
CH ₃ CN	396	560	7395	37,50	1,3441	0,305416
DMSO	412	568	6666	46,70	1,4783	0,263401

**Figure 10.** Effect of solvents on the photophysical properties of compound **3zh**.**Figure 11.** Lippert-Mataga plot.

fluorescence spectra of compound **3zh** was obtained in the presence of 21 metal ions (Li⁺, Na⁺, K⁺, Ca²⁺, Mg²⁺, Ba²⁺, Al³⁺,

Cr³⁺, Cu²⁺, Fe²⁺, Ag⁺, Cd²⁺, Co²⁺, Hg²⁺, Mn²⁺, Ni²⁺, Pb²⁺, Zn²⁺, Ga³⁺, In³⁺, Y³⁺) at various concentrations. An obvious quenching of the fluorescence was noted upon the addition of the rare-earth metal ions Ga³⁺, In³⁺ and Y³⁺ to the solution of styrylisoxazole **3zb** in acetonitrile without a shift of the emission maximum. An example of the fluorescence spectrum of compound **3zh** upon the addition of various amounts of Y(NO₃)₃ is shown in Figure S8 (see SI).

Biological activity

We also tested the cytotoxicity of a series of 5-styrylisoxazoles using MTT test. For compounds **3k**, **3o**, **3p**, **3t**, **3zg**, **3zh** and **3zk** the activity against MCF-7 (breast carcinoma), HCT-116 (colon carcinoma), A549 (pulmonary carcinoma) and WI38 (fibroblasts from lung tissue) was studied. Screening of the selected compounds revealed their moderate cytotoxicity with IC₅₀ values in the range from 10 to 100 μM. Compound **3t** turned out to be the most cytotoxic in relation to both cancer and conditionally normal cells (10–25 μM). At the same time, compound **3zh** with the highest quantum yield did not show toxicity, what can find application for the use in biological imaging (Table 4).

Apoptosis, or programmed cell death, is interrupted in cancer cells, and cellular parameter is commonly measured in cancer drug screening. To demonstrate that this cell death mechanism is realized for studied compounds, the impact of 5-styrylisoxazole **3t** on early and late apoptosis levels in HCT116 cells was examined using the Muse[®] AnnexinV & Dead Cell Kit by flow cytometry.^[17] Cells were incubated with compound and cisplatin for 48 h at concentrations corresponding to 2xIC₅₀ values. It was shown that compound **3t** intensely induces apoptosis, wherein the percentage of Annexin V-positive cells for **3t** in the late apoptosis is significantly higher than with cisplatin: 13.8 ± 1.5% and 1.38 ± 0.7%, respectively (see Figure S9 and S10, SI).

Caspases serve an important function in a process of apoptosis in response to proapoptotic signals. Effector caspases direct cellular breakdown through cleavage of structural proteins (Caspase-3/7). The activation of caspases 3/7 was studied on the example of compound **3t** by flow cytometry with the Muse[®] Caspase-3/7 Kit, and it was found that this heterocycle activated caspases 3/7 more effectively than cisplatin, as can be seen from Figure S5. Activation of caspases is considered an essential event during apoptosis and is regularly

Table 4. Results of MTT assay for selected 5-styrylisoxazoles on different cell lines.

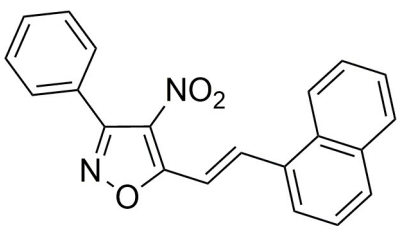
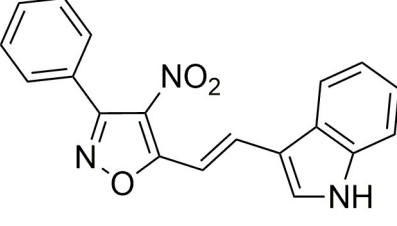
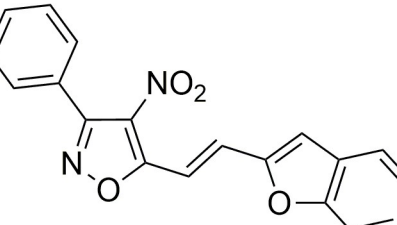
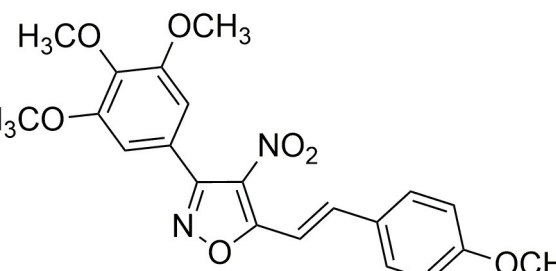
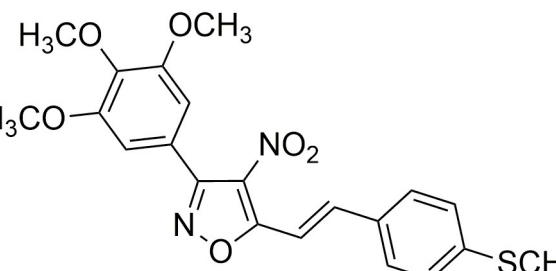
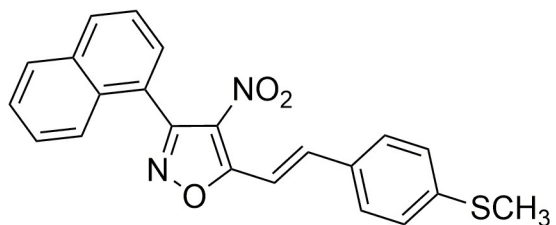
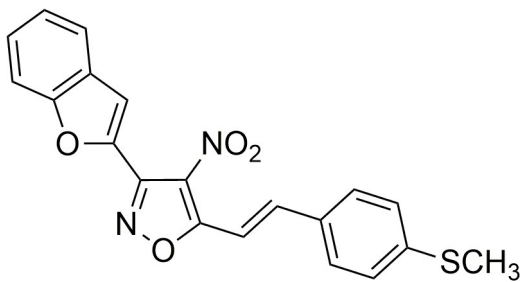
Compounds	Structure	IC ₅₀ [μM]			
		MCF-7	HCT-116	A549	WI38
3k		44.6 ± 5	57.2 ± 11.3	45.3 ± 10	61 ± 15
3o		63.2 ± 15	22.3 ± 4.5	125.1	165.1
3p		75.6 ± 13	60.4 ± 25	> 200	67.4 ± 20
3t		53.5 ± 12	20.6 ± 4.3	35.8 ± 9	86.7 ± 16
3zg		25.5 ± 6.7	9.8 ± 3.1	24.7 ± 7.5	17.1 ± 3
3zh		> 200	95.8 ± 17.1	> 200	> 200

Table 4. continued		IC ₅₀ [μM]			
Compounds	Structure	MCF-7	HCT-116	A549	WI38
		3zk		> 200	39.7 ± 19.4
Cisplatin		15.5 ± 3	8.3 ± 3.5	10.4 ± 1.5	5.5 ± 0.5

used for the preclinical toxicity screening of anticancer compound. To visualize the activity of compound **3t** in caspase activation, the fluorescent kit CellEvent™ Caspase-3/7 Green ReadyProbes™ Reagent was applied. After incubation of HCT 116 cells with compound **3t**, the kit reagent was added and the formation of bright green fluorescent cells with activated caspases was observed (Figure S11).

Conclusion

In summary, two large series of novel π -conjugated 5-styrylisoxazoles with varying aryl/hetaryl substituents at position 3 of the isoxazole cycle and in styryl moiety were synthesized and their photophysical properties were investigated. It was found that the longest wavelength absorption bands maxima of 5-styrylisoxazoles lay in UV-visible region, and the most of compounds exhibit pronounced fluorescence in blue, green or yellow-green regions with large Stokes shifts. Photophysical data and DFT calculations reveal that 4-nitroisoxazole and styryl moieties are effectively conjugated, whilst 3-aryl/hetaryl fragments weakly contribute to the π -conjugated system of styrylisoxazoles. Also, it was shown that positive emission solvatochromism and chemosensor properties are observed for 5-styrylisoxazoles. Taking into account the potential biological activity and cytotoxicity of isoxazole derivatives, this structural type of heterocycles is of interest for medicinal chemistry and can be further used to create fluorescent labels based on them.

Experimental Section

General Information: NMR spectra were recorded on spectrometer Bruker Avance 400 and Agilent 400-MR (400.0 MHz for ¹H; 100.6 MHz for ¹³C; 376.3 MHz for ¹⁹F) at r. t.; the chemical shifts δ were measured in ppm with respect to the CDCl₃ (¹H: δ = 7.26 ppm, ¹³C: δ = 77.16 ppm), DMSO-d₆ (¹H: δ = 2.50 ppm, ¹³C: δ = 39.52 ppm) and CFC₃ as external standard for ¹⁹F. Chemical shifts (δ) are given in ppm; J values are given in Hz. When necessary, assignments of signals in NMR spectra were made using 2D techniques. Accurate mass measurements (HRMS) were performed on a Bruker micrOTOF II instrument using electrospray ionization (ESI). The measurements

were done in a positive ion mode (interface capillary voltage 4500 V) or in a negative ion mode (3200 V). Melting points (mp) are uncorrected. Thin layer chromatographic method (TLC) was conducted on DC-Fertigfolien ALUGRAM pre-coated silica gel 60-F254 plates; the detection was done by UV lamp (254 and 365 nm) and chemical staining (5% aqueous solution of KMnO₄). Column chromatography was performed on silica gel (230–400 mesh, Merck).

Ultraviolet/Visible spectra were obtained on Agilent Cary 60 spectrophotometer. Fluorescence spectra in solutions were recorded on Hitachi F2700 fluorescence spectrophotometer.

Fluorescence quantum yield (\pm 10%) determined relative to quinine sulfate in 0.05M H₂SO₄ (ψ = 53%) and rhodamine-G in ethanol for **3e** (ψ = 94%) as standards.^[18] Fluorescence intensity decays were obtained by time-correlated single photoncounting measurements in CH₂Cl₂ at 25 °C at $c \approx 10^{-5}$ M. Excitation wavelength – 360 nm.

Aromatic aldehyde (tert-butyl 2-formyl-1H-pyrrole-1-carboxylate,^[19] 1-methyl-1,2,3,4-tetrahydroquinoline-6-carbaldehyde,^[20] benzofuran-2-carbaldehyde,^[21] naphtho[2,1-b]furan-2-carbaldehyde,^[21] 6-methoxybenzofuran-2-carbaldehyde,^[22] were synthesized by described methods from commercial products.

β -Arylsubstituted vinylketones were **1a**, **1b**, **1c**, **1d**, **1e**, **1f**, **1g**, **1h** synthesized by Wittig reaction in DCM at 20 °C,^[23] **1i**, **1m**, **1j**, **1l**, **1k**, **1o** synthesized by Wittig reaction in toluene at 80 °C.^[24]

All 4-nitroisoxazoles **2a–o** were synthesized by discovered by our method^[11] based on the reaction of heterocyclization of the corresponding α,β -unsaturated ketones **1a–o** upon the treatment with t-BuONO.

All other starting materials were commercially available. All reagents except commercial products of satisfactory quality were purified by literature procedures prior to use.

General procedure for compounds 3a–3k, 3m–3r, 3s, 3u–3w, 3y, 3za–3zc, 3zh–3zj: To a solution of the corresponding 4-nitroisoxazole **2** (0.2 mmol) in EtOH (1 mL) aromatic aldehyde (0.2 mmol) and few drops of piperidine were added. The resulting mixture was stirred at 25 °C for 12 h. Formed precipitate was filtered and washed by cold EtOH. The obtained product required no additional purification.

5-[(E)-2-[4-(Methylthio)phenyl]vinyl]-3-(1-naphthyl)-4-nitroisoxazole (3 zh)

Yellow solid; yield: 57 mg (74 %); mp: 209–211 °C. $^1\text{H NMR}$ (400 MHz, CDCl_3): δ 2.55 (s, 3H, CH_3S), 7.29–7.34 (m, 2H, 2CH(Ar)), 7.47–7.65 (m, 7H, 7CH(Ar)), 7.74 (d, $^3J=16.5$ Hz, 1H, CH=), 7.90 (d, $^3J=16.5$ Hz, 1H, CH=), 7.93–7.97 (m, 1H, CH(Ar)), 8.02–8.07 (m, 1H, CH(Ar)); $^{13}\text{C NMR}$ (100 MHz, CDCl_3): δ 15.2 (CH_3S), 109.9 (CH=), 123.9 (C(Ar)), 124.6 (CH(Ar)), 125.1 (CH(Ar)), 126.1 (2CH(Ar)), 126.6 (CH(Ar)), 127.3 (CH(Ar)), 128.28 (CH(Ar)), 128.34 (CNO₂), 128.8 (CH(Ar)), 129.0 (2CH(Ar)), 131.0 (C(Ar)), 131.1 (CH(Ar)), 131.7 (C(Ar)), 133.5 (C(Ar)), 143.1 (CH=), 143.9 (C(Ar)), 158.0 (C), 167.8 (C). **HRMS** (ESI): m/z [M+Na]⁺ calcd for $\text{C}_{22}\text{H}_{16}\text{N}_2\text{O}_3\text{SNa}^+$: 411.0774; found: 411.0769. The remaining spectral data are provided in the supplementary file.

General procedure for the synthesis of compounds 3i, 3t, 3x, 3z, 3zd–3zf, 3zg, 3zk: To a solution of the corresponding 4-nitroisoxazole 2 (0.2 mmol) in EtOH (1 mL) aromatic aldehyde (0.2 mmol) and few drops of piperidine were added. The resulting mixture was stirred at 80 °C for 2 h and then cooled down to room temperature. Formed precipitate was filtered and washed by cold EtOH. The obtained product required no additional purification.

3-Biphenyl-4-yl-5-[(E)-2-(4-methoxyphenyl)vinyl]-4-nitroisoxazole (3 z)

Yellow solid; yield: 64 mg (80 %); mp: 201–203 °C. $^1\text{H NMR}$ (400 MHz, CDCl_3): δ 3.89 (s, 3H, CH_3O), 6.96–7.02 (m, 2H, 2CH(Ar)), 7.37–7.44 (m, 1H, CH(Ar)), 7.45–7.52 (m, 2H, CH(Ar)), 7.60 (d, $^3J=16.5$ Hz, 1H, CH=), 7.63–7.69 (m, 4H, 4CH(Ar)), 7.71–7.76 (m, 4H, 4CH(Ar)), 7.84 (d, $^3J=16.5$ Hz, 1H, CH=); $^{13}\text{C NMR}$ (100 MHz, CDCl_3): δ 55.7 (CH_3O), 108.6 (CH=), 114.9 (2CH(Ar)), 125.1 (C(Ar)), 126.8 (CNO₂), 127.3 (2CH(Ar)), 127.4 (3CH(Ar)), 128.1 (C(Ar)), 129.1 (2CH(Ar)), 130.0 (2CH(Ar)), 130.5 (2CH(Ar)), 140.3 (C(Ar)), 143.3 (CH=), 143.6 (C(Ar)), 158.3 (C), 162.4 (C(Ar)), 168.7 (C). **HRMS** (ESI): m/z [M+H]⁺ calcd for $\text{C}_{24}\text{H}_{19}\text{N}_2\text{O}_4^+$: 399.1339; found: 399.1337. The remaining spectral data are provided in the supplementary file.

X-ray Crystallography

Deposition Numbers 2259479 (for **3zb**) and 2259480 (for **3zh**) contain the supplementary crystallographic data for this paper. These data are provided free of charge by the joint Cambridge Crystallographic Data Centre and Fachinformationszentrum Karlsruhe Access Structures service www.ccdc.cam.ac.uk/structures.

Supporting Information Summary

Supporting Information (SI) available: Experimental Section with complete characterization data of compounds, copies of the ^1H , ^{13}C , and 2DNMR spectra, procedures of biological evaluation and data of DFT calculations.

Author contributions

Conceptualization, D.A.V. and E.B.A.; software, D.A.V.; investigation, K.S.S., Yu.A.G., Yu.K.G., V.A.R., V.A.T., N.E.A., and I.D.B.; writing – original draft preparation, D.A.V. and K.S.S.; writing – review and editing, D.A.V., and E.B.A.; visualization, K.S.S., D.A.V.,

Ya.A.G., V.A.T., N.E.A., I.D.B.; supervision, E.B.A. and E.R.M.; funding acquisition, D.A.V.

Acknowledgements

This work was supported by Russian Science Foundation (project 22-73-00058 (synthesis of **3zh**, the study of the solvatochromism, photostability, cytotoxicity; X-Ray analysis) and project 19-73-00145 (synthesis of compounds **1**, **2**, **3**, the study emission, fluorescent and sensor properties, quantum chemical calculations)). The kinetic of fluorescent decay was carried out in the Core Facility of the Institute of Biochemical Physics RAS “New Materials and Technologies” and was supported by the RF State Program for IBCP RAS, Project no. 1201253303.

Conflict of Interests

The authors declare no conflict of interest.

Data Availability Statement

The data that support the findings of this study are available in the supplementary material of this article.

Keywords: Fluorescence · Isoxazole · Styryl dyes · Solvatochromism · Cytotoxicity

- [1] a) F. Hu, M. Szostak, *Adv. Synth. Catal.* **2015**, *357*, 2583–2614; b) S. Fuse, T. Morita, H. Nakamura, *Synthesis* **2017**, *49*, 2351–2360; c) D. A. Vasilenko, K. N. Sedenkova, T. S. Kuznetsova, E. B. Averina, *Synthesis* **2019**, *51*, 1516–1528; d) T. Morita, S. Yugandar, S. Fuse, H. Nakamura, *Tetrahedron Lett.* **2018**, *59*, 1159–1171.
- [2] a) J. Zhu, J. Mo, H. Lin, Y. Chen, H. Sun, *Bioorg. Med. Chem.* **2018**, *26*, 3065–3075; b) A. Sysak, B. Obmińska-Mrukowicz, *Eur. J. Med. Chem.* **2017**, *137*, 292–309; c) E. Vitaku, D. T. Smith, J. T. Njardarson, *J. Med. Chem.* **2014**, *57*, 10257–10274.
- [3] a) M. A. Kalwat, Z. Huang, C. Wichaidit, K. McGlynn, S. Earnest, C. Savoia, E. M. Dioum, J. W. Schneider, M. R. Hutchison, M. H. Cobb, *ACS Chem. Biol.* **2016**, *11*, 1128–1136; b) J. Kaffy, R. Pontikis, D. Carrez, A. Croisy, C. Monneret, J.-C. Florenta, *Bioorg. Med. Chem.* **2016**, *14*, 4067–4077; c) D. A. Vasilenko, E. V. Dueva, L. I. Kozlovskaya, N. A. Zefirov, Y. K. Grishin, G. M. Butov, V. A. Palyulin, T. S. Kuznetsova, G. G. Karganova, O. N. Zefirova, D. I. Osolodkin, E. B. Averina, *Bioorg. Chem.* **2019**, *87*, 629–637; d) R. Wu, W. Ding, T. Liu, H. Zhu, Y. Hu, B. Yang, Q. He, *Cancer Lett.* **2009**, *285*, 13–22; e) G. N. Pairas, F. Perperopoulou, P. G. Tsoungas, G. Varvounis, *ChemMedChem* **2017**, *12*, 408–419; f) C. Zhang, X. Wang, H. Liu, M. Zhang, M. Geng, L. Sun, A. Shen, A. Zhang, *Eur. J. Med. Chem.* **2017**, *125*, 315–326; g) M. L. Herrmann, R. Schleyerbach, B. J. Kirschbaum, *Immunopharmacology* **2000**, *47*, 273–289; h) D. Simoni, R. Rondanin, R. Baruchello, M. Rizzi, G. Grisolia, M. Eleopra, S. Grimaudo, A. D. Cristina, M. R. Pipitone, M. R. Bongiorno, M. Arico, F. P. Invidiata, M. Tolomeo, *J. Med. Chem.* **2008**, *51*, 4796–4803; i) M. Eda, T. Kuroda, S. Kaneko, Y. Aoki, M. Yamashita, C. Okumura, Y. Ikeda, T. Ohbora, M. Sakaue, N. Koyama, K. Aritomo, *J. Med. Chem.* **2015**, *58*, 4918–4926; j) K. S. Sadovnikov, D. A. Vasilenko, K. N. Sedenkova, V. B. Rybakov, Y. K. Grishin, V. A. Alferova, T. S. Kuznetsova, E. B. Averina, *Mendeleev Commun.* **2020**, *30*, 487–489; k) M. Zimecki, U. Bąchor, M. Mączyński, *Molecules* **2018**, *23*, 2724–2741; l) M. Mączyński, J. Artych, M. Kocięba, I. Kochanowska, S. Ryng, M. Zimecki, *Pharmacol. Rep.* **2016**, *68*, 894–902; m) K. S. Sadovnikov, D. A. Vasilenko, Y. A. Gracheva, N. A. Zefirov, E. V. Radchenko, V. A. Palyulin, Y. K. Grishin, V. A. Vasilichin, A. A. Shtil, P. N. Shevtsov, E. F. Shevtsova, T. S. Kuznetsova, S. A. Kuznetsov, A. S. Bunev, E. R. Milaeva, E. B. Averina, *Arch. Pharm.* **2022**, *355*, e2100425; n) D. A. Vasilenko, E. B. Averina, N. A. Zefirov, B. Wobith, Y. K. Grishin, V. B.

- Rybakov, O. N. Zefirova, T. S. Kuznetsova, S. A. Kuznetsov, N. S. Zefirov, *Mendeleev Commun.* **2017**, *27*, 228–230; o) E. B. Averina, D. A. Vasilenko, Y. A. Gracheva, Y. K. Grishin, E. V. Radchenko, V. V. Burmistrov, G. M. Butov, M. E. Neganova, T. P. Serkova, O. M. Redkozubova, E. F. Shevtsova, E. R. Milaeva, T. S. Kuznetsova, N. S. Zefirov, *Bioorg. Med. Chem.* **2016**, *24*, 712–720.
- [4] a) V. Sharma, J. Kaur, S. S. Chimni, *Eur. J. Org. Chem.* **2018**, *2018*, 3489–3495; b) M. Moccia, R. J. Wells, M. F. A. Adamo, *Org. Biomol. Chem.* **2015**, *13*, 2192–2195; c) S. Rout, H. Joshi, V. K. Singh, *Org. Lett.* **2018**, *20*, 2199–2203; d) M. Moccia, M. Cortigiani, C. Monasterolo, F. Torri, C. D. Fiandra, G. Fuller, B. Kelly, M. F. A. Adamo, *Org. Process Res. Dev.* **2015**, *19*, 1274–1281; e) X.-W. Liu, Z. Yao, G.-L. Wang, Z.-Y. Chen, X.-L. Liu, M.-Y. Tian, Q.-D. Wei, Y. Zhou, J.-F. Zhang, *Synth. Commun.* **2018**, *48*, 1454–1464; f) M. Cortigiani, A. Tampieri, C. Monasterolo, A. Mereu, M. F. A. Adamo, *Tetrahedron Lett.* **2017**, *58*, 4205–4208.
- [5] a) X.-L. Liu, Q.-D. Wei, X. Zuo, S.-W. Xu, Z. Yao, J.-X. Wang, Y. Zhou, *Adv. Synth. Catal.* **2019**, *361*, 2836–2843; b) P. Chauhan, S. Mahajan, G. Raabe, D. Enders, *Chem. Commun.* **2015**, *51*, 2270–2272; c) S. Nagaraju, K. Sathish, N. Satyanarayana, B. Paplal, D. Kashinath, *J. Heterocycl. Chem.* **2020**, *57*, 469–476; d) X.-L. Liu, W.-Y. Han, X. M. Zhang, W.-C. Yuan, *Org. Lett.* **2013**, *15*, 1246–1249; e) B. Zhu, B. Lu, H. Zhang, X. Xu, Z. Jiang, J. Chang, *Org. Lett.* **2019**, *21*, 3271–3275; f) Q. D. Wei, Y.-M. Yao, S.-Q. Chang, W.-D. Yang, M.-Y. Tian, X.-L. Liu, Y. Zhou, *Synthesis* **2020**; *52*, 85–97.
- [6] a) X.-Y. Chen, S. Li, H. Sheng, Q. Liu, E. Jafari, C. Essen, K. Rissanen, D. Enders, *Chem. Eur. J.* **2017**, *23*, 13042–13045; b) K. Liu, Y. Xiong, Z.-F. Wang, H.-Y. Tao, C.-J. Wang, *Chem. Commun.* **2016**, *52*, 9458–9461; c) J. Liao, J. Dong, J. Xu, W. Wang, Y. Wu, Y. Hou, H. Guo, *J. Org. Chem.* **2021**, *86*, 2090–2099; d) S. Kato, Y. Suzuki, K. Suzuki, R. Haraguchi, S. Fukuzawa, *J. Org. Chem.* **2018**, *83*, 13965–13972; e) X. Zhang, X. Xu, D. Zhang, *Molecules* **2017**, *22*, 1131–1142; f) M. S. Reddy, N. S. Kumar, L. R. Chowhan, *RSC Adv.* **2018**, *8*, 35587–35593; g) M. S. Reddy, L. R. Chowhan, N. S. Kumar, P. Ramesh, S. B. Mukkamala, *Tetrahedron Lett.* **2018**, *59*, 1366–1371; h) X.-W. Liu, Z. Yao, J. Yang, Z.-Y. Chen, X.-L. Liu, Z. Zhao, Y. Lu, Y. Zhou, Y. Cao, *Tetrahedron* **2016**, *72*, 1364–1374.
- [7] a) X.-Y. Chen, Q. Liu, P. Chauhan, S. Li, A. Peuronen, K. Rissanen, E. Jafari, D. Enders, *Angew. Chem. Int. Ed.* **2017**, *56*, 6241–6245; b) Y. Li, F. J. López-Delgado, D. K. B. Jørgensen, R. P. Nielsen, H. Jiang, K. A. Jørgensen, *Chem. Commun.* **2014**, *50*, 15689–15691.
- [8] a) F. Bureš, *RSC Adv.* **2014**, *4*, 58826–58851; b) T. Deligeorgiev, A. Vasilev, S. Kaloyanova, J. J. Vaquero, *Color. Technol.* **2010**, *126*, 55–80; c) M.-C. Chen, D.-G. Chen, P.-T. Chou, *ChemPlusChem* **2021**, *86*, 11–27.
- [9] a) A. Saady, E. Varon, A. Jacob, Y. Shav-Tal, B. Fischer, *Dyes Pigm.* **2020**, *174*, 107986; b) Y. Li, T. Liu, H. Liu, M.-Z. Tian, Y. Li, *Acc. Chem. Res.* **2014**, *47*, 1186–1198; c) L. Zhang, X. Liu, S. Lu, J. Liu, S. Zhong, Y. Wei, T. Bing, N. Zhang, D. Shangguan, *ACS Appl. Bio Mater.* **2020**, *3*, 2643–2650; d) M. Collot, E. Boutant, K. T. Fam, L. Danglot, A. S. Klymchenko, *Bioconjugate Chem.* **2020**, *31*, 875–883; e) T. Deligeorgiev, A. Vasilev, S. Kaloyanova, J. J. Vaquero, *Color. Technol.* **2010**, *126*, 55–80; f) V. D. Gupta, V. S. Padalkar, K. R. Phatangare, V. S. Patil, P. G. Umape, N. Sekar, *Dyes Pigm.* **2011**, *88*, 378–384; g) K. Avhad, A. Jadhav, N. Sekar, *J. Chem. Sci.* **2017**, *129*, 1829–1841; h) T. Venugopal, J. Palanivel, J. Jayaraman, *J. Phys. Org. Chem.* **2017**, *30*, e3695; i) U. N. Yadav, H. S. Kumbhar, S. S. Deshpande, S. K. Sahoo, G. S. Shankarling, *RSC Adv.* **2015**, *5*, 42971–42977.
- [10] J. Katla, S. Kanvah, *Photochem. Photobiol. Sci.* **2018**, *17*, 42–50.
- [11] D. A. Vasilenko, K. S. Sadovnikov, K. N. Sedenkova, A. V. Kurova, Y. K. Grishin, T. S. Kuznetsova, V. B. Rybakov, Y. A. Volkova, E. B. Averina, *Synthesis* **2020**, *52*, 1398–1406.
- [12] F. Neese, Software update: the ORCA program system, version 4.0. *WIREs Comput. Mol. Sci.* **2018**, *8*, e1327.
- [13] F. Weigend, R. Ahlrichs, *Phys. Chem. Chem. Phys.* **2005**, *7*, 3297–3305.
- [14] H. Güsten, D. Schulte-Frohlinde, *Chem. Ber.* **1971**, *104*, 402–406.
- [15] E. Lippert, *Ber. Bunsen-Ges.* **1957**, *61*, 962–975.
- [16] a) N. M. Karayannis, C. M. Mikulski, S. D. Sonsino, E. E. Bradshaw, L. L. Pytlewski, *Inorg Chim Acta* **1975**, *14*, 195–200; b) W. L. Driessen, P. H. Voort, *Inorg Chim Acta* **1977**, *21*, 217–222; c) S. Madhavan, S. K. Keshri, M. Kapur, *Asian J. Org. Chem.* **2021**, *10*, 3127–3165.
- [17] I. Vermes, C. Haanen, H. Steffens-Nakken, C. Reutellingsperger, *J. Immunol. Methods* **1995**, *184*, 39–51.
- [18] A. M. Brouwer, *Pure Appl. Chem.* **2011**, *83*, 2213–2228.
- [19] T. Flack, C. Romain, A. J. P. White, P. R. Haycock, A. Barnard, *Org. Lett.* **2019**, *21*, 4433–4438.
- [20] a) B. S. Rauckman, M. Y. Tidwell, J. V. Johnson, B. Roth, *J. Med. Chem.* **1989**, *32*, 1927–1935; b) R. J. Mayer, N. Hampel, P. Mayer, A. R. Ofial, H. Mayr, *Eur. J. Org. Chem.* **2019**, *2019*, 412–421.
- [21] H. Langhals, S. Pust, *Chem. Ber.* **1986**, *118*, 4674–4681.
- [22] W. Chen, Z.-H. Zhou, H.-B. Chen, *Org. Biomol. Chem.* **2017**, *15*, 1530–1536.
- [23] F. Pesciaoli, F. Vincenti, P. Galzerano, G. Bencivenni, G. Bartoli, A. Mazzanti, P. Melchiorre, *Angew. Chem. Int. Ed.* **2008**, *47*, 8703–8706.
- [24] J.-L. Shih, T. S. Nguyen, J. A. May, *Angew. Chem. Int. Ed.* **2015**, *54*, 9931–9935.

Submitted: March 3, 2023

Accepted: May 8, 2023